Penerbit Akademia Baru

Journal of Advanced Research in Fluid Mechanics and Thermal Sciences

Journal homepage: www.akademiabaru.com/arfmts.html
ISSN: 2289-7879

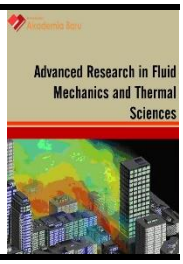

Computational Fluid Dynamics Study of Cricket Ball Aerodynamics Associated With Swing

Open Access

Sagar Kalburgi[1], Ashwini Rathi[2], Mukund Narayan[2], Laxmikant G. Keni[2], Chethan K.N.[2], Mohammad Zuber[2,*]

[1] Aerospace Department, Indian Institute of Science, Bengaluru, Karnataka, India
[2] Department of Aeronautical Engineering, Manipal Institute of Technology, MAHE, Manipal, Karnataka, India

ARTICLE INFO

Article history:
Received 29 March 2020
Received in revised form 25 June 2020
Accepted 25 June 2020
Available online 15 September 2020

Keywords:
Computational Fluid Dynamics; Cricket ball aerodynamics; Swing; Flow separation

ABSTRACT

The lateral deviation of the cricket ball, often named as 'Swing', is one of the most complex phenomena in the sport of cricket. As the ball proceeds through the flight path, the interaction between the ball surface and flow field causes a deviation for the ball from the initial path, resulting in a modified curved path. Several experimental tests have been conducted to study the parameters which cause the 'swing' phenomenon, in order to improve and optimize the performance of the cricket ball. A seam is a governing factor for the magnitude of swing. This is attributed to the considerable difference in the pressure acting on the seam and non-seam side of the ball which, consequently, produces the side force. In this work, a computational fluid dynamic modeling for the cricket ball in the flow field has been carried out. The Flow field at 0° and 20° seam angles and four bowling velocities of 5, 25, 29, and 36.5 m/s have been computationally analyzed. The pressure difference across the ball at 0° seam angle has no significant effect for producing any observable swing. The maximum pressure difference was achieved at the velocity of 29 m/s, and, generally, the speed above 30 m/s does not affect the swing**.** As the flow velocity increases above 30m/s, asymmetric pressure distribution can be noticed but with a negligible effect as in the lower velocities. Thus, the optimum swing can be obtained only at velocities below 30 m/s.

1. Introduction

Cricket is one of the games that has infinite possibilities, not just in strategy and gameplay, but also, in its basic aerodynamic mechanism [1]. In addition, it involves a lot of undiscovered complex mechanics that distinguishes between the good and average player [2]. A single ball delivery has millions of probabilities for flight path based on the delivery speed, trajectory taken, spin if it is given

* *Corresponding author.*
E-mail address: mohammad.zuber@manipal.edu

https://doi.org/10.37934/arfmts.75.2.125136

to the ball (Magnus Effect) [3], bowling pace, length, and line, etc. With an increase in popularity of the game, several studies [3–5] involving aerodynamics, ball material, optimal techniques of the ball swing have been carried out. Mehta *et al.,* [6] experimentally studied the causes and the effects of the cricket ball swing, and also, the concepts of reverse swing. Cooke *et al.,* [7] considered as the pioneer in the field of the scientific study of the cricket ball. They investigated the 'swerve' phenomenon associated with the new ball and the difficulties associated with the harder ball when the shine has worn off it. Mehta *et al.,* [5,8] have immensely contributed to study the science and various manoeuvres of a cricket ball. Their study involved the calculation of the magnitudes of side forces and the parameters that resulted in the aerodynamic manoeuvring throughout the flight path. Later, Bown *et al.,* [9], in the 1980's and 90's, talked for the first time about the concept of "Reverse Swing". CFD-based studies using finite element analysis techniques were conducted by Cheng *et al.,* [10-11]. Moreover, the prediction of the flow field around the cricket ball along with some calculations of the aerodynamic forces on a spinning ball were conducted [12-13]. James *et al.,* [14] studied the release conditions that swing bowlers impart to the ball which, also, can be used as the initial conditions for the model.

Mehta *et al.,* [15] conducted an experimental study to calculate the surface pressure distribution across a cricket ball. Experimental results were still not in agreement with what was actually observed on a cricket ground. This discrepancy was solved by Verma *et al.,* [16] and Da Silva *et al.,* [17]. The indirect method of measuring side force was held responsible by Da Silva *et al.,* for these inaccuracies. They performed a more detailed analysis and used direct measurement techniques to get a maximum swing on a new cricket ball at 35m/s for a seam angle of 100. Despite several studies, accurate depiction of swing and its fundamental extrapolation was not possible experimentally. Computational Fluid dynamics-based analysis is a useful tool to determine the pressure acting on any point on the ball surface. It not only helps estimate the pressure gradients but also visualizes the flow regions and flow separation around the cricket ball. Computational fluid dynamics is a powerful tool in which flow analysis can be performed [18-19].

In the present study, the effect of various seam angles on the cricket ball is carried out using computational fluid dynamic analysis. The analysis was accomplished for the cricket ball at 0° and 20° seem angle. The pressure coefficients were estimated and validated with the existing literature. The outcome of this study is expected to benefit a better understanding of the seam motion of the cricket ball and benefit the sport for further advancement.

2. Methodology

2.1 Modeling

The current model was based on the data of the actual cricket ball documented in Mehta [5]. The model was designed in CATIA V-6. For installing pressure probes internally, the primary seam with six rows of stitching adjacent to each other was modelled, as shown in Figure 1. More often, in a better quality ball for competitive matches, one can find a secondary seam with internal hemispherical stitching layers. Usually, the three major layers of a cricket ball are cork-rubber core in the centre with a package of cork-twine and a cover of the stitched layer. These materials influence the speed and bowling rate of a cricket ball [4]. The stitches and the size of the hemispheres were taken into account and modelled accurately in this study. The seam and the aerodynamic after-effects are the main point of discussion in the current paper.

The major aerodynamic flow visualization patterns on a cricket ball due to the presence of seam at a defined approximate angle to the initial flight velocity vector results in a peculiar curved path

[20]. This can be captured by pressure taps. Hence, modelling of these aspects with high precision was of utmost importance.

This was achieved by making holes along the ball surface on the plane perpendicular to the stitches as presented in the experiment of Mehta *et al.,* [15]. Each tap was of 1 mm in diameter and was modelled around the ball perpendicular to the plane of the seam and spaced by 15° from the next tap.

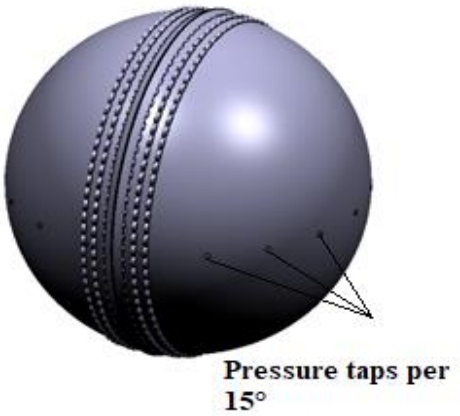

Fig. 1. Isometric view of ball geometry with 24 pressure taps spaced by 15° from each other

2.2 Meshing

After the completion of designing the ball in CATIA V-6, it was then modelled with ANSYS Fluent 19 R1. Meshing, with effective in-built geometric elements, plays a critical role in the accuracy of predicting the necessary boundary-flow interaction between the ball and the surrounding fluid [11]. The mesh is unstructured with dense, finer elements at the surface of the ball. The mesh density in the domain region is less dense, with coarse elements compared to the surface.

A close-up view of the mesh developed is shown in Figure 2.

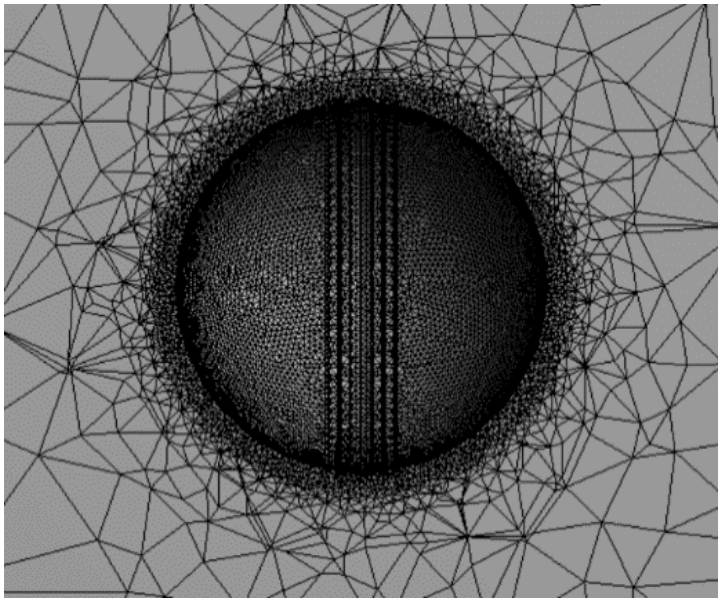

Fig. 2. Mesh distribution pattern

2.3 Boundary Conditions and Solution Steps

The setting of the boundary conditions is one of the most crucial parts of the simulation. In this study, flow velocities at 0° and 20° seam angle to the line of flight were applied as in the experimental work of Mehta *et al.,* [15]. The velocities for which the pressure coefficients were calculated are 5 m/s, 25 m/s, 29 m/s, and 36.5 m/s. The solution was iterated for convergence criteria of 10^{-6}.

In order to minimize the computation time and increase the accuracy, firstly, a mesh independency study was conducted. Three different mesh densities were developed and tested. The maximum and minimum pressure coefficient values for each pressure ports were investigated to specify the mesh applied in the current study. The results of this test are shown in Table 1.

Table 1
Pressure co-efficient at different density mesh sizes

Mesh	Max. Pressure Co-efficient	Min. Pressure. Co-efficient
Coarse	1.07	-1.21
Medium	1.01	-1.20
Fine	0.98	-1.23

Considering the runtime and processing power for the medium and fine mesh, the error in pressure coefficient values seemed to be < 3%. Therefore, the medium mesh was adopted for further analysis and calculations.

2.4 Governing Equations

The Direct Numerical Simulation (DNS) and Reynolds-Averages Naiver-Stokes equations (RANS) can be used to solve the eddy viscosity field in the current study. However, the much more processing time that may be consumed by DNS motivated the authors to use RANS. Non-linear second order differential equations for turbulent viscous flow boundary governed by the Naiver-Stokes equations are presented in the following section. The Reynolds number in the flow analysis accomplished in this work ranges from 23700 to 173000. The turbulent nature of the flow can be amplified due to seam, in which the flow stream adheres to the surface causing delayed separation when compared to the laminar flow on the non-seam side. Usage of the k-ε model is required to obtain the solution for two-scale eddy viscosity.

Solution of two-scale eddy viscosity problem in the outer region can be solved using the two-equation K-ε model, while the solution for near-wall viscosity problem can be solved using one-equation k-model.

Here, K is turbulent kinetic energy with scalar dissipation rate of turbulent kinetic energy ε.

2.4.1 One-equation turbulent model:

The partial differential equations to be solved for the calculation of $\overline{u}_i$ mean-velocity, $\overline{p}$ average pressure and *K* [21].

$$\frac{\partial K}{\partial t} + \overline{u}_i \frac{\partial K}{\partial x_i} = -\tau_{ij} \frac{\partial \overline{u}_i}{\partial x_j} - C^* \frac{K^{\frac{3}{2}}}{l_o} + \frac{\partial}{\partial x_i}\left(\frac{v_T}{\sigma_K} \frac{\partial K}{\partial x_i}\right) + v \frac{\partial^2 K}{\partial x_i \partial x_i} \quad (1)$$

$$\tau_{ij} = \frac{2}{3} K \delta_{ij} - v_T \left(\frac{\partial \overline{u}_i}{\partial x_j} + \frac{\partial \overline{u}_j}{\partial x_i}\right) \quad (2)$$

$$v_T = K^{1/2} l_o \tag{3}$$

$\sigma_K \cong 1.0$ is a non-dimensional constant.
C^*= 0.166 is a non-dimensional constant.
τ_{ij} Reynold's stress term, v fluid kinematic viscosity, l_o is the turbulence length scale factor.

2.4.2 Two-equation K- ε model

The difference between the one-equation and two-equation model is, in the two-equation model, two separate sets of transport equations are solved for two independent turbulent quantities (K- ε), directly related to the turbulence length and time scales.

The system of partial differential equations to be solved for the calculation of $\overline{u}_i$ mean-velocity, $\overline{p}$ average pressure, *K and* ε [21].

$$\frac{\partial K}{\partial t} + \overline{u}_i \frac{\partial K}{\partial x_i} = -\tau_{ij} \frac{\partial \overline{u}_i}{\partial x_j} - C^* \frac{K^{\frac{3}{2}}}{l_o} + \frac{\partial}{\partial x_i}\left(\frac{v_T}{\sigma_K} \frac{\partial K}{\partial x_i}\right) + v \frac{\partial^2 K}{\partial x_i \partial x_i} \tag{4}$$

$$\frac{\partial \epsilon}{\partial t} + \overline{u}_i \frac{\partial \varepsilon}{\partial x_i} = -C_{\epsilon 1} \frac{\epsilon}{K} \tau_{ij} \frac{\partial \overline{u}_i}{\partial x_j} + \frac{\partial}{\partial x_i}\left(\frac{v_T}{\sigma_\epsilon} \frac{\partial \epsilon}{\partial x_i}\right) - C_{\epsilon 2} \frac{\epsilon^2}{K} + v \frac{\partial^2 \epsilon}{\partial x_i \partial x_i} \tag{5}$$

$$\tau_{ij} = \frac{2}{3} K \delta_{ij} - v_T \left(\frac{\partial \overline{u}_i}{\partial x_j} + \frac{\partial \overline{u}_j}{\partial x_i}\right) \tag{6}$$

$$v_T = C_\mu \frac{K^2}{\epsilon} \tag{7}$$

Based on the comparison with physical experiments, the constants assume the values.
$C_{\epsilon 1} = 1.44, \quad C_{\epsilon 2} = 1.92, \quad C_\mu = 0.09, \quad \sigma_\epsilon = 1.3$

3. Results

Figure 3 represents the distribution of the pressure coefficients (C_P) for the four tested bowling speeds at 0° and 20° seam angle. Three pressure taps P 6, P 7, and P 8 on the left hemisphere, three other taps P 18, P 19, and P 20 on the right hemisphere were chosen to determine the significance of pressure difference across the ball. Here, the average C_P, and hence, the average pressure for the three consecutive pressure taps were accounted for both hemispheres. Accordingly, the pressure difference (Δp) across the ball can be obtained from Figure 3, as listed in Table 2. This pressure difference per unit area results in the side force that causes swing.

The results of Table 2 shows that the pressure difference obtained at 5m/s is very negligible as this speed represents very low Re number. Therefore, the pressure difference across the ball at 0° seam angle has no significant effect for producing any observable swing. Another observation is that, at the highest velocity (36.5m/s), the asymmetric pressure distribution around the ball also does not produce any significant pressure changes when compared with the corresponding changes in the velocity range between 25m/s to 30m/s.

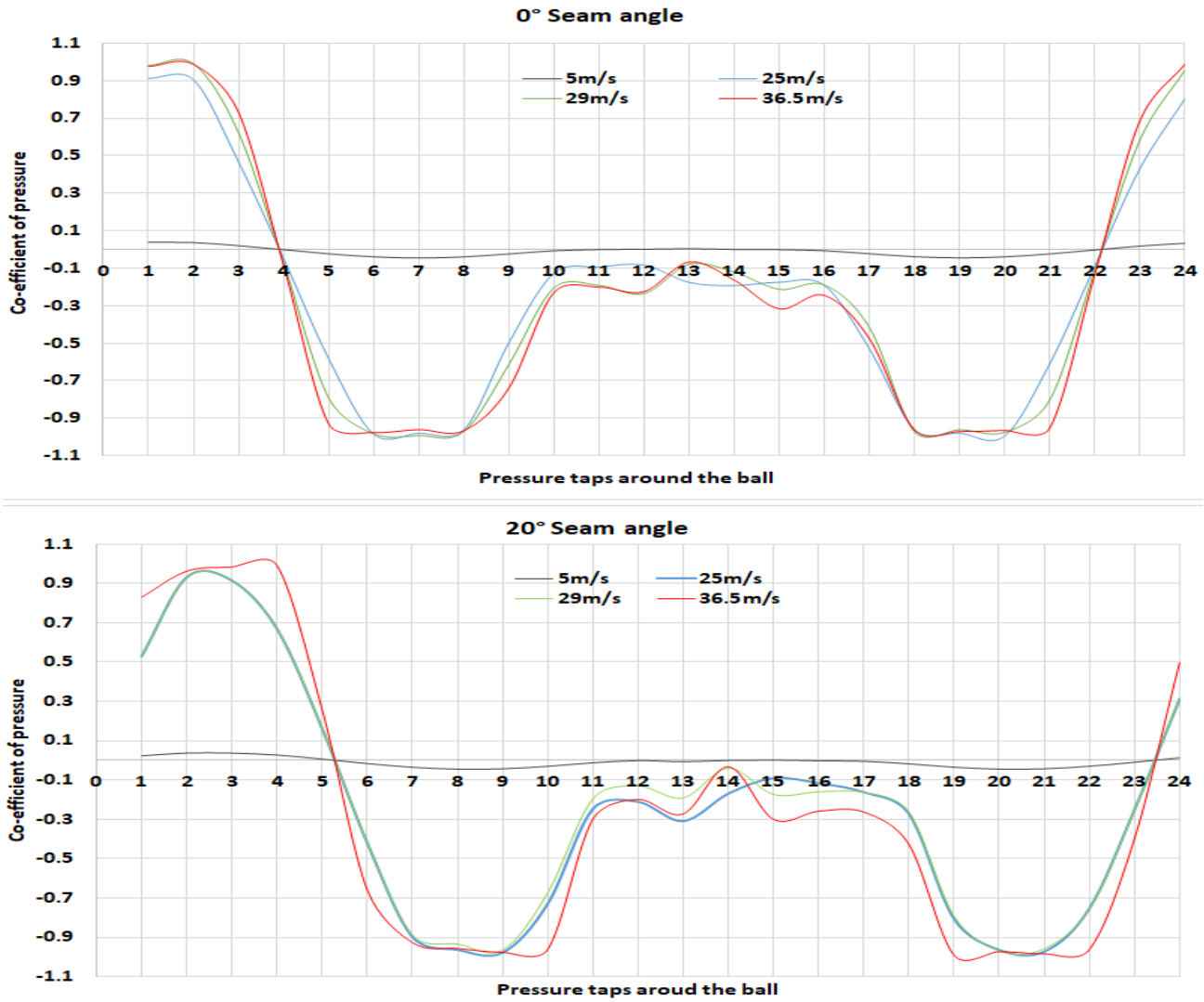

Fig. 1. Pressure coefficient distribution at four balling speeds at 0° and 20° seam angle

Table 2
The magnitude of pressure difference per unit area

Velocity (m/s)	ΔP at 0° seam	ΔP at 20° seam
5	0.00054	0.00043
25	0.00233	0.06400
29	0.01267	0.07133
36.5	0.00133	0.05100

Bowling speed and seam angle are the factors causing asymmetric pressure difference. This pressure difference then produces the side force, hence swing. In the present study, 29m/s is proved to be the optimal ball speed for efficient swing as a result of a maximum pressure difference. This is consistency with the findings reported by Mehta *et al.,* [15].

Figure 4 depicts two pressure difference curves, one at the 0° seam and the other at 20° seam angle. Through this graph, the role of the seam angle of the ball with the flight path line to produce significant pressure difference can be noted.

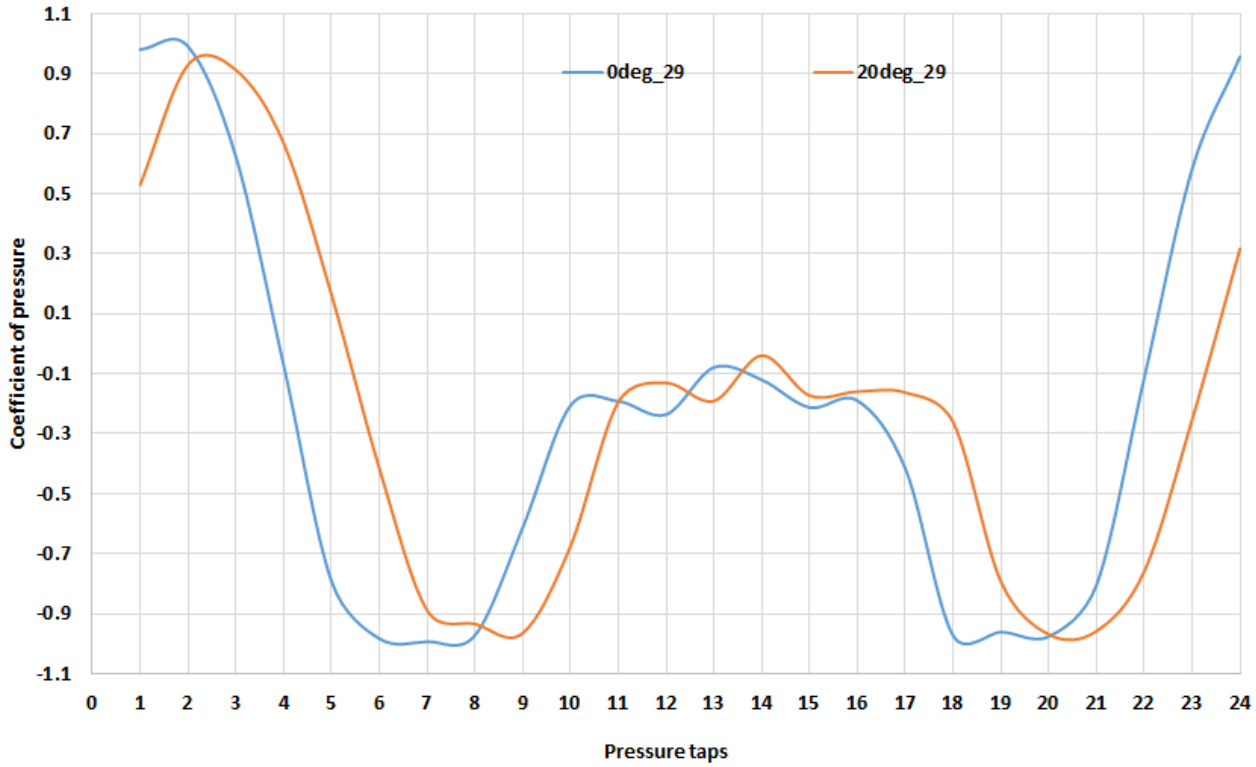

Fig. 2. Pressure difference at 0° and 20° seam angle for velocity 29 m/s

Figure 5 shows a graphical representation for comparing the pressure distribution at both 0° and 20° seam at 29 m/s bowling speed. The left side of each figure represents the pressure distribution at the pressure taps from 1 to 12, whereas the pressure distribution at the taps from 13 to 24 is displayed in the right side.

It can be seen from Figure 5(a) that the pressure distribution is symmetric around the ball. There is no unbalanced side force acting on the seam surface. As a consequence, no swing will be generated at 0° seam angle. Figure 5(b) shows the pressure distributed for a 20° seam angle. A clear asymmetric pressure distribution pattern can be observed at this angle. This side force helps in deviating the straight flight path to a curvilinear path which causes the swing motion of the ball. This shows that the seam angle is the primary driver of the swing phenomenon.

Pressure contours in the flow regime around the ball during the flight path are shown in Figure 6.

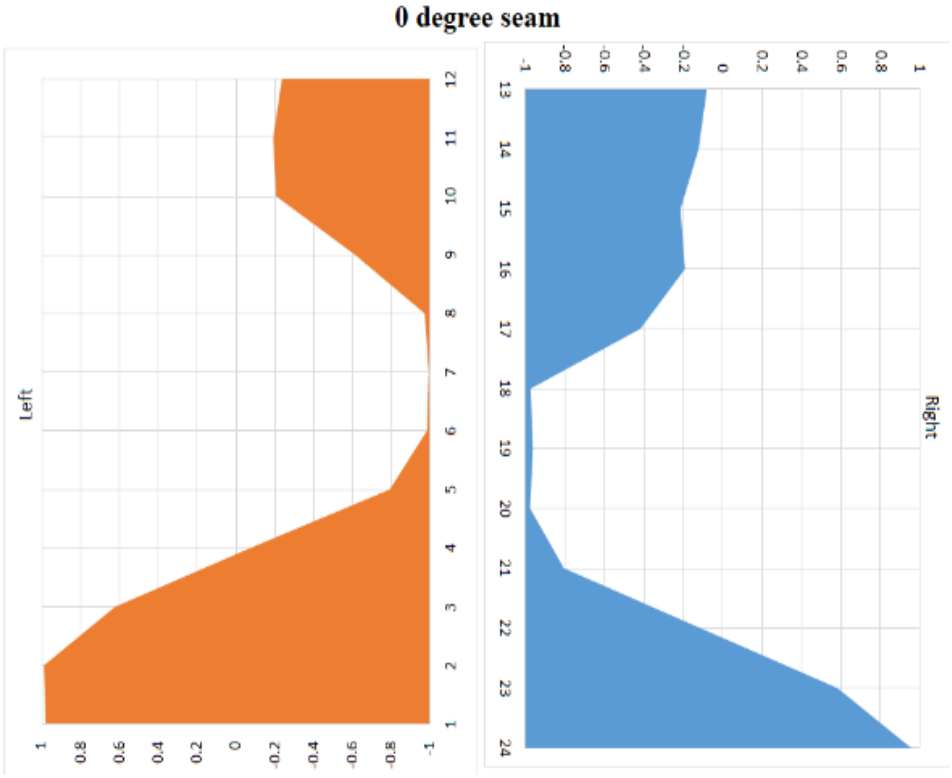

(a)

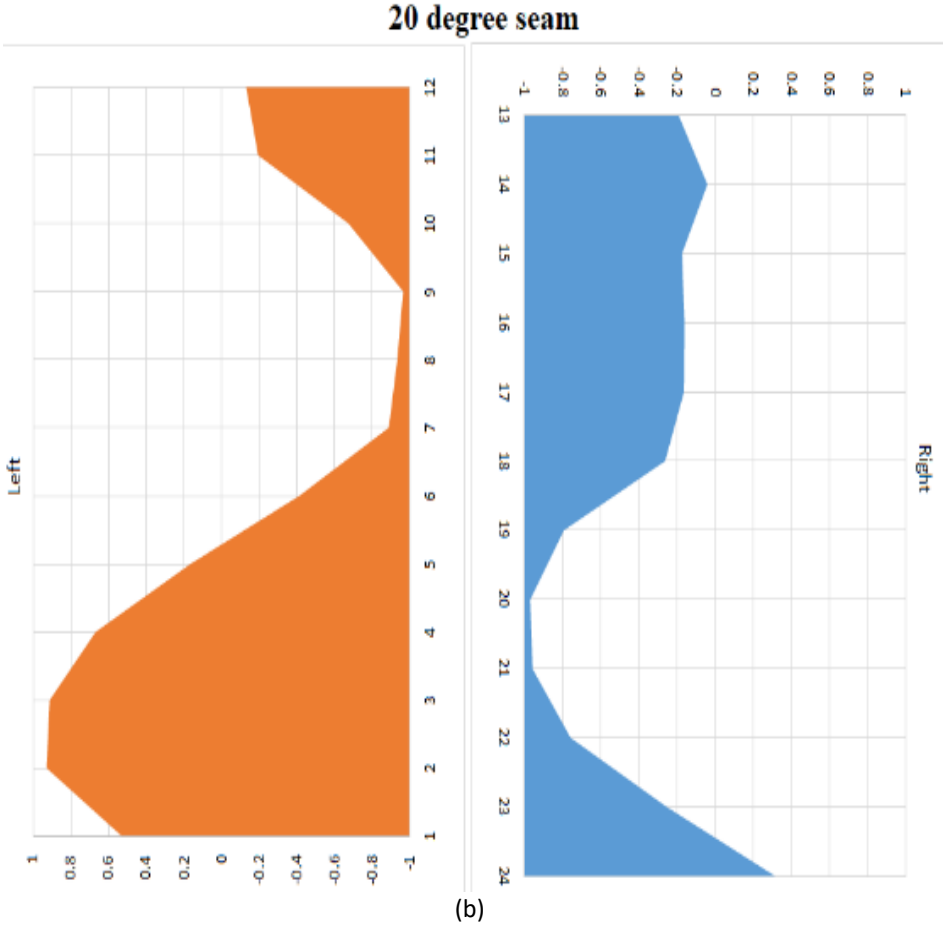

(b)

Fig. 5. A graphical representation of the pressure distribution for (a) 0° seam and (b) 20° seam

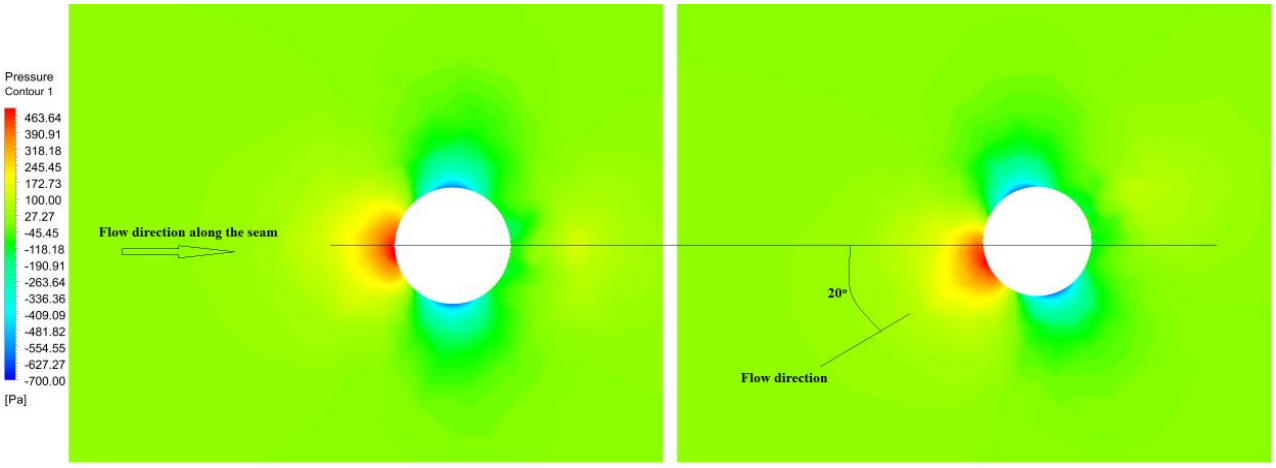

Fig. 6. Comparison between pressure contour at 0° and 20° seam to the line of flight at 29m/s

Figure 7 and 8 represent the flow separation points at 0° and 20° seam angle. In Figure 8, on non-seam side the early flow separation point in the laminar region is noticed, while at the same time on the seam side, seam trips the laminar flFow to turbulent. This turbulent flow causes delay in the flow separation from surface of the ball, hence creating a low-pressure zone on the seam side.

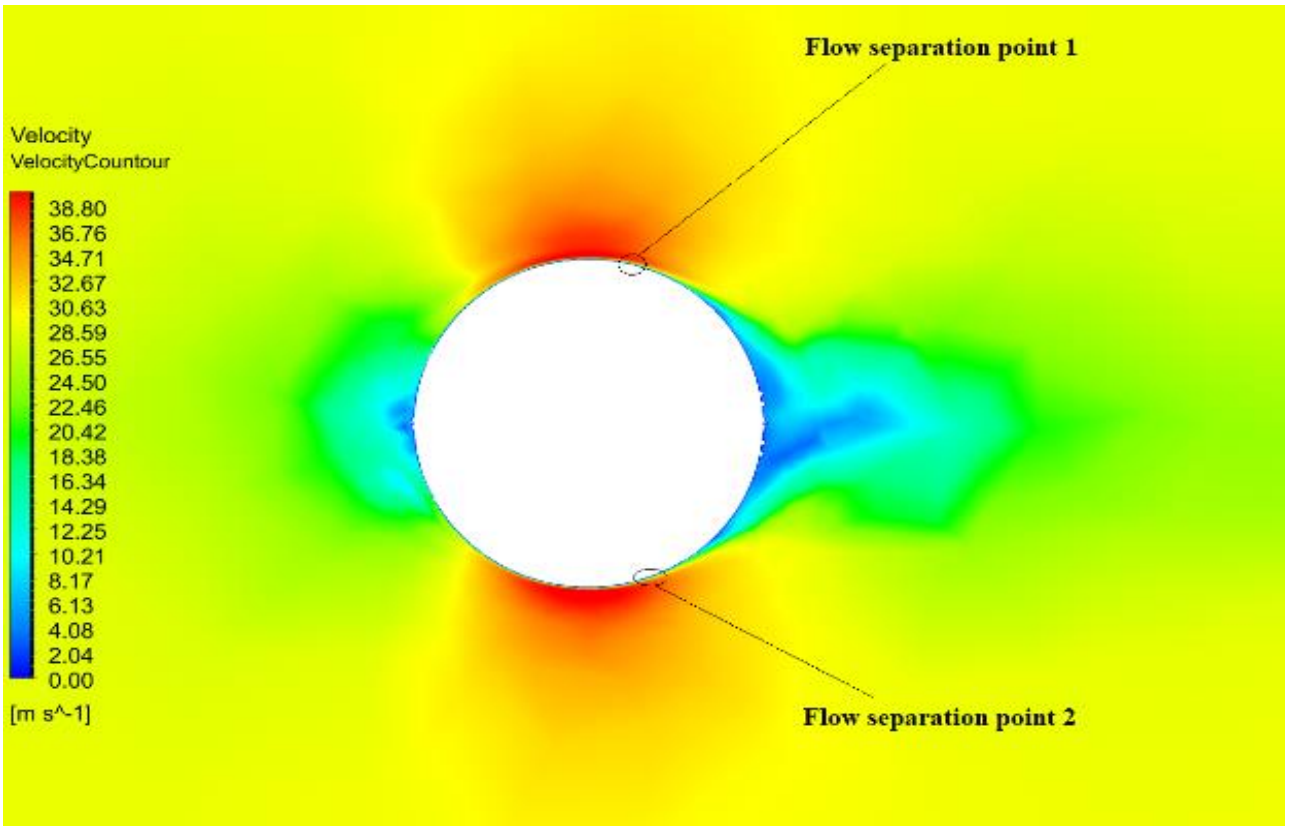

Fig. 7. Velocity contour depicting the flow separation point at 0° seam

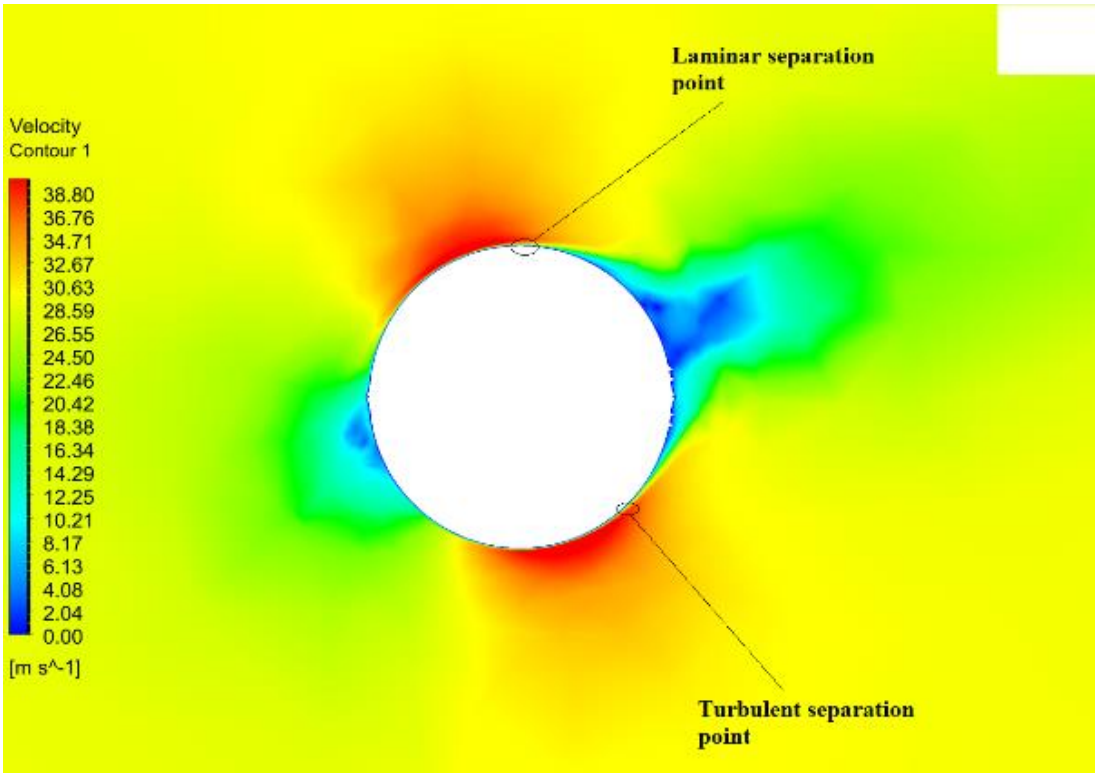

Fig. 8. Velocity contour depicting the flow separation point at 20° seam

4. Discussion

This paper aims to re-emphasize one of Mehta's findings. Their practical experiment on a cricket ball imparted a study on calculating the surface pressure distribution across a cricket ball [15]. The experiment was carried out in wind tunnel with ball mounted at 20° seam to the line of flight. Twenty-four pressure taps along the ball surface, perpendicular to the seam plane were installed on the cricket ball subjected to four inflow velocities of 5, 25, 29, and 36.5 m/s. Injection of smoke to capture wake formations as a result of asymmetric laminar and turbulence boundary layer separation due to seam geometry, causing pressure gradient. The resulting pressure distributions captured in the pressure taps were then plotted with angle around the ball along X-axis and pressure coefficient on the Y-axis.

According to Mehta *et al.,* [15], the effect of side force at velocity U = 5 m/s is very negligible. As the magnitude of side force is proportional to pressure distribution, the low pressure difference at this velocity results in a minute side force. This was established in the present work. At U= 25 m/s, the ball will swing to the seam side because of the presence of laminar flow over the non-seam side. While on the seam side, the seam trips the laminar flow to the turbulent flow resulting in the asymmetric pressure gradient causing the side force as can been seen from Figures 6(a) and 6(b).

The maximum pressure difference was achieved at U=29 m/s, as demonstrated from Table 2. Seam is a governing factor for the magnitude of swing. This is attributed to the considerable difference in the pressure acting on seam and non-seam side of the ball which, consequently, produces the side force. This is similar to the results of Mehta *et al.,* [15]. As the flow velocity increases above 30m/s, asymmetric pressure distribution can be noticed but with a negligible effect as in the lower velocities. Thus, the optimum swing can be obtained only at velocities below 30 m/s. This shows that the swing phenomenon can be estimated as a function of bowling speed and seam angle. Additionally, it can optimally occur at a certain operating velocity. Some of the other factors, namely surface roughness and weather conditions on-field [14] also have a consequence on the flight

path of the swing. Surface roughness involves skin friction drag consideration, as a result, the futuristic studies can purely be based on wall-stresses around the ball surface in the projectile and skin-friction drag regime.

5. Conclusion

From the above findings, it can now be established that critical factors necessary to define the efficiency, direction, and magnitude of ball swing are bowling speed and seam angle to the velocity vector or line of flight. Swing relies on an asymmetry of flow within the boundary layer on either side of the ball. Bowlers orientate the ball such that the main seam trips the boundary layer on one side of the ball, therefore one might hypothesize that a subtly larger seam may create more asymmetry, and thus, more swing.

Acknowledgement

The authors thank the Department of Aeronautical and Automobile Engineering, Manipal Institute of Technology, Manipal Academy of Higher Education, Manipal for providing the high computational facility to carry out this research.

References

[1] Alam, Firoz, Harun Chowdhury, and Hazim Moria. "A review on aerodynamics and hydrodynamics in sports." *Energy Procedia* 160 (2019): 798-805. https://doi.org/10.1016/j.egypro.2019.02.158

[2] Worthington, Peter J., Mark A. King, and Craig A. Ranson. "Relationships between fast bowling technique and ball release speed in cricket." *Journal of applied biomechanics* 29, no. 1 (2013): 78-84. https://doi.org/10.1123/jab.29.1.78

[3] Fuss, Franz Konstantin, Robert Masterton Smith, and Aleksandar Subic. "Determination of spin rate and axes with an instrumented cricket ball." *Procedia Engineering* 34 (2012): 128-133. https://doi.org/10.1016/j.proeng.2012.04.023

[4] A.J. Subic, and A.J. Cooke. *Materials in cricket*. Woodhead Publishing Limited, 2003. https://doi.org/10.1533/9781855738546.2.342

[5] Mehta, Rabindra D. "An overview of cricket ball swing." *Sports Engineering* 8, no. 4 (2005): 181-192. https://doi.org/10.1007/BF02844161

[6] Mehta, R. D., K. Bentley, M. Proudlove, and P. Varty. "Factors affecting cricket ball swing." *Nature* 303, no. 5920 (1983): 787-788. https://doi.org/10.1038/303787a0

[7] Cooke, J. C. "The Boundary Layer and" Seam" Bowling." *The Mathematical Gazette* 39, no. 329 (1955): 196-199. https://doi.org/10.2307/3608746

[8] Mehta, Rabindra D. "Aerodynamics of sports balls." *Annual Review of Fluid Mechanics* 17, no. 1 (1985): 151-189. https://doi.org/10.1146/annurev.fl.17.010185.001055

[9] Bown, William, and Rabi Mehta. "The seamy side of swing bowling-English cricket faces another humiliating test match this week, but could some long-forgotten research restore its flagging fortunes?." *New Scientist-UK Edition* 139, no. 1887 (1993): 21-24.

[10] Cheng, Ning. "Development of a universal FE model of a cricket ball." (2009).

[11] Cheng, Ning, Monir Takla, and Aleksandar Subic. "Development of an FE model of a cricket ball." *Procedia Engineering* 13 (2011): 238-245. https://doi.org/10.1016/j.proeng.2011.05.079

[12] Subic, A. J. "The Engineering of Sport Research, Development and." (2000).

[13] Sayers, A. T., and A. Hill. "Aerodynamics of a cricket ball." *Journal of Wind Engineering and Industrial Aerodynamics* 79, no. 1-2 (1999): 169-182. https://doi.org/10.1016/S0167-6105(97)00299-7

[14] James, David, Danielle C. MacDonald, and John Hart. "The effect of atmospheric conditions on the swing of a cricket ball." *Procedia engineering* 34 (2012): 188-193. https://doi.org/10.1016/j.proeng.2012.04.033

[15] Mehta, R. D. "Fluid mechanics of cricket ball swing." In *19th Australasian fluid mechanics conference*. 2014.
[16] Verma, Saumitra. "A Review on the Swing of a Cricket Ball KEYWORDS: Boundary Layer Theory, Swing, Seam Angle, Surface Roughness." *IJSR - INTERNATIONAL JOURNAL OF SCIENTIFIC RESEARCH* 4, no.1 (2015): 420-424.
[17] Shrivastava, G. S. "On the Swing ofa Cricket Ball." *West Indian Journal of Engineering* 24, no. 1 (2001): 25-34.
[18] Dandan, Muhammad Arif, Syahrullail Samion, Mohamad Nor Musa, and Fazila M. Zawawi. "Evaluation of Lift and Drag Force of Outward Dimple Cylinder Using Wind Tunnel." *CFD Letters* 11, no. 3 (2019): 145-153.
[19] Huang, Lim Gim, Normayati Nordin, Lim Chia Chun, Nur Shafiqah Abdul Rahim, Shamsuri Mohamed Rasidi, and Muhammad Zahid Firdaus Shariff. "Effect of Turbulence Intensity on Turning Diffuser Performance at Various Angle of Turns." *CFD Letters* 12, no. 1 (2020): 48-61.
[20] Lock, Gary D., S. Edwards, and Darryl P. Almond. "Flow visualization experiments demonstrating the reverse swing of a cricket ball." *Proceedings of the Institution of Mechanical Engineers, Part P: Journal of Sports Engineering and Technology* 224, no. 3 (2010): 191-199.
https://doi.org/10.1243/17543371JSET73
[21] Alfonsi, Giancarlo. "Reynolds-averaged Navier–Stokes equations for turbulence modeling." *Applied Mechanics Reviews* 62, no. 4 (2009).
https://doi.org/10.1115/1.3124648